STATENS GEOTEKNISKA INSTITUT

SWEDISH GEOTECHNICAL INSTITUTE

No. 20

SÄRTRYCK OCH PRELIMINÄRA RAPPORTER

REPRINTS AND PRELIMINARY REPORTS

Supplement to the "Proceedings" and "Meddelanden" of the Institute

Contributions to the First Congress of the International Society of Rock Mechanics, Lisbon 1966.

1. A Note on Strength Properties of Rock
   by Bengt Broms

2. Tensile Strength of Rock Materials
   by Bengt Broms

STOCKHOLM 1967

STATENS GEOTEKNISKA INSTITUT

SWEDISH GEOTECHNICAL INSTITUTE

No. 20

SÄRTRYCK OCH PRELIMINÄRA RAPPORTER

REPRINTS AND PRELIMINARY REPORTS

Supplement to the ''Proceedings'' and ''Meddelanden'' of the Institute

Contributions to the First Congress of the International Society of Rock Mechanics, Lisbon 1966.

1. A Note on Strength Properties of Rock
   by Bengt Broms

2. Tensile Strength of Rock Materials
   by Bengt Broms

Reprinted from the Proceedings of the First Congress of the International Society of Rock Mechanics, Lisbon 1966, Vol, 2 and Vol. 3, respectively.

STOCKHOLM 1967

A note on strength properties of rock

Notice sur les propriétés de résistance d'une roche

Bemerkung über die Scherfestigkeitseigenschaften eines Felsens

by BENGT B. BROMS
Director, Swedish Geotechnical Institute, Stockholm, Sweden

Summary

A method is proposed by which the shear strength of a rock can be expressed in terms of a cohesion c_m and a friction angle ϕ_m. It is shown *a*) that these shear strength parameters are functions of the strain level in the rock, *b*) that the maximum cohesion c_m is not necessarily mobilized at the same axial deformation as the friction angle ϕ_m and *c*) that the maximum bearing capacity or penetration resistance cannot as a rule be predicted by using the maximum value of the cohesion c_m and the maximum value of the friction angle ϕ_m.

The use of the shear strength parameters c_m and ϕ_m is illustrated by a numerical example.

Résumé

On propose une méthode par laquelle la résistance au cisaillement d'une roche peut être exprimée en fonction de la cohésion c_m et de l'angle de frottement ϕ_m. Il est démontré que *a*) ces paramètres de résistance au cisaillement sont des fonctions du niveau de déformation de la roche, que *b*) la cohésion maximum c_m n'est pas nécessairement mobilisée à la même déformation axiale que l'angle de frottement ϕ_m et que *c*) la capacité portante maximum ou résistance à la pénétration ne peut être prévue, en règle générale, en utilisant la valeur maximum de la cohésion c_m et la valeur maximum de l'angle de frottement ϕ_m.

L'emploi des paramètres de résistance au cisaillement c_m et ϕ_m est illustré par un exemple numérique.

Zusammenfassung

Es wird ein Verfahren vorgeschlagen, um die Scherfestigkeit von Felsen durch die Kohäsion c_m und den Winkel der inneren Reibung ϕ_m auszudrücken. Es wird gezeigt, dass *a*) diese Parameter der Scherfestigkeit Funktionen von Deformationsniveau im Felsen sind, *b*) die maximale Kohäsion c_m nicht notwendigerweise bei derselben Axialdeformation wie der Winkel der inneren Reibung ϕ_m mobilisiert wird und *c*) die maximale Tragfähigkeit oder der Eindringungswiderstand meistens nicht durch Benutzung des Höchstwertes der Kohäsion c_m und des Höchstwertes des Winkels der inneren Reibung ϕ_m vorhergesagt werden kann.

Die Anwendung der Parameter der Scherfestigkeit c_m und ϕ_m ist an einem numerischen Beispiele erläutert.

Introduction

The shear strength s of rock material along a surface of failure is frequently expressed in terms of a cohesive strength c and a friction coefficient tan ϕ expressed by the Coulomb-Mohr equation:

$$s = c + \bar{p} \tan \phi$$

where $\bar{p}$ is the effective stress acting on the plane of failure. The cohesion c is defined as that part of the total shearing resistance which is independent of the normal effective pressure acting on the failure plane. The friction coefficient tan ϕ expresses the relationship between friction resistance and effective normal pressure acting on the plane of failure.

The shear strength parameters c and ϕ are generally determined from a series of triaxial tests carried out at different confining pressures. Typical stress-strain relationships are shown in Fig. 1. It can be seen that both the peak strength (the stress corresponding to the peak point of the stress-strain relationship) and the strain corresponding to the peak strength increase rapidly with increasing confining pressure. The Mohr's stress circles corresponding to the peak strengths are shown in Fig. 2. The centre of each stress circle is located on the horizontal axis at a distance of $\frac{1}{2}(p_1 + p_3)$ from the origin. In this expression p_1 is the measured peak strength and p_3 the applied confin-

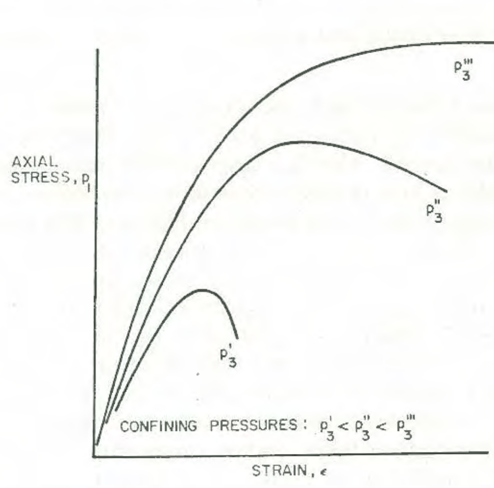

Figure 1 — Typical stress-strain relationships for chosen confining pressures

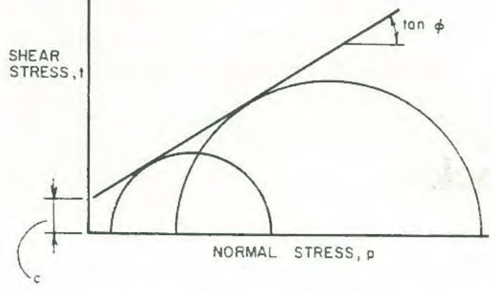

Figure 2 — Mohr's stress circles

ing pressure. The inclination of the envelope curve to the stress circle and the intercept of the envelope curve with the vertical shear axis of the Mohr diagram are commonly said to be equal to tan ϕ and the cohesion c, respectively.

Interpretation of triaxial tests

The shear strength parameters c and ϕ determined in this manner are frequently used to predict the behavior of a rock mass under load. For example, the parameters c and ϕ have been used to calculate the penetration resistance of a wedge which is forced into a rock mass at relatively high fluid pressures. From a knowledge of the load-penetration relationships at different configurations, it is possible to predict, for example, the drilling performance of rotary bits under different drilling conditions.

In the calculations of the penetration resistance of a wedge, it is frequently assumed that rock behaves as an ideal plastic material with a stress-strain relationship as shown in Fig. 3. Thus, it is frequently assumed that the

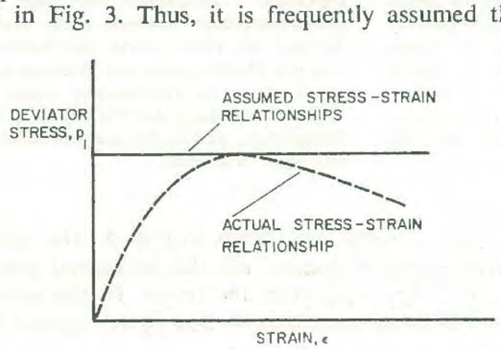

Figure 3 — Actual and assumed stress-strain relationships

maximum cohesion and the maximum friction resistance are mobilized at failure at every point along the failure or rupture surface. This is a questionable assumption. The magnitude of the normal stress along the failure surface is very high close to the wedge surface and this stress decreases rapidly with increasing distance from the wedge. It can be seen from Fig. 1 that the unit deformation required to mobilize the maximum shear resistance corresponding to the peak strength is higher close to the wedge (where the normal stresses are high) than at some distance from the wedge (where the normal stresses are relatively low). Thus, it is not likely that the maximum shear resistance is fully mobilized at failure (when a rock chip breaks loose) along the entire failure surface. A hypothesis is presented in this paper which takes into account the possible variation of shear resistance along the failure surface. It can be shown by this method that the real penetration resistance will be considerably less than that calculated from the parameters c and ϕ.

Mobilized cohesion and angle of internal friction

The shear resistance mobilized during a triaxial test depends on the applied axial deformation and on the applied confining pressure. The axial stress which corresponds to the axial strain ε_1 will be p'_1, p''_1 and p'''_1 at the three confining pressures p'_3, p''_3 and p'''_3, respectively, as shown in Fig. 4. Thus, it can be seen that the axial stress required to deform a test sample to the same axial deformation will increase with increasing confining pressure.

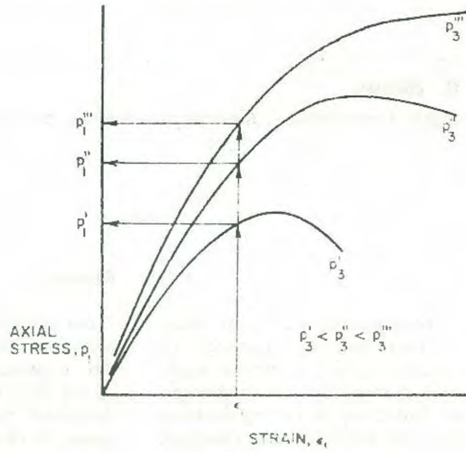

Figure 4 — Mobilized shear resistance

The shear resistance mobilized at a certain axial deformation can be evaluated from a series of Mohr's stress circles as shown in Fig. 5. The stress circles shown in this figure correspond to a constant axial strain which is equal to ε_1. The slope of the envelope curve to these stress circles is equal to the angle of internal friction ϕ'_m which is mobilized at the axial strain ε_1 and the intercept of this envelope curve with the vertical shear stress axial is equal to the cohesion c'_m which is mobilized at the axial strain ε_1. Usually, the envelope curve is not straight. In this case, the average slope of the envelope curve for the pressure range considered should be used in the analysis of the test data.

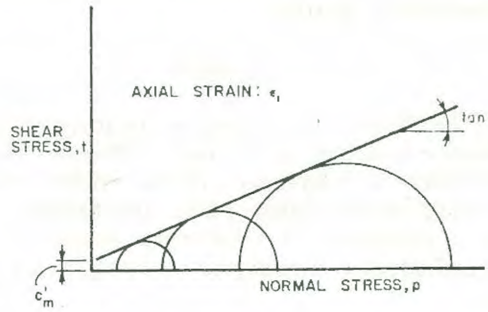

Figure 5 — Evaluation of c'_m and ϕ'_m

The friction angle ϕ_m and the cohesion c_m will both be a function of the axial strain ε. These relationships can be determined from the slopes and the intercept of the envelope curves constructed at different axial deformations. The relationships determined in this manner are

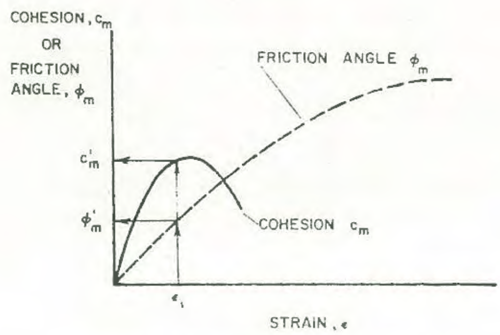

Figure 6 — Mobilization of c_m and ϕ_m

shown in Fig. 6. It can be seen that the mobilized cohesion c_m increases very rapidly with increasing axial deformations and reaches a maximum value at a relatively small axial deformation. The friction resistance $\bar{p}$ tan ϕ_m increases relatively slowly with increasing axial deformations and reaches a maximum at a relatively large axial deformation.

The strain corresponding to the peak of a particular stress-strain curve will generally not coincide with either the strain at which the peak cohesion is mobilized or the strain at which the peak angle of internal friction is mobilized. The peak point of a particular stress-strain relationship will correspond to the strain at which the sum of the mobilized cohesion and the mobilized friction resistance reaches a maximum.

Penetration resistance of a wedge

The mobilized cohesion c_m and the mobilized friction resistance tan ϕ_m can be used to predict the penetration resistance of a wedge. The theoretical slip line pattern

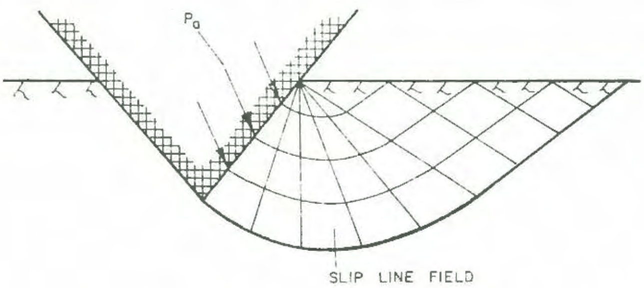

Figure 7 — Slip line field for a wedge

for a rough wedge which is pushed into a rock mass is shown in Fig. 7. As the wedge penetrates into the rock mass, the contact pressure p_a will increase as the deformation of the rock surrounding the wedge increases.

The contact pressure p_a can be expressed in terms of the mobilized cohesion c_m and the friction resistance ϕ_m if the deformations of the rock are known or assumed. These calculations become relatively simple if it is assumed that the deformations are uniformly distributed. For this particular case, the penetration resistance can be calculated directly from Fig. 6 as a function of an equivalent axial strain. At the equivalent axial strain ε_1, the cohesion c'_m and the friction angle ϕ'_m are mobilized. With a knowledge of these two quantities, the penetration resistance can be calculated. The resulting relationship between penetration resistance and equivalent axial deformation is shown in

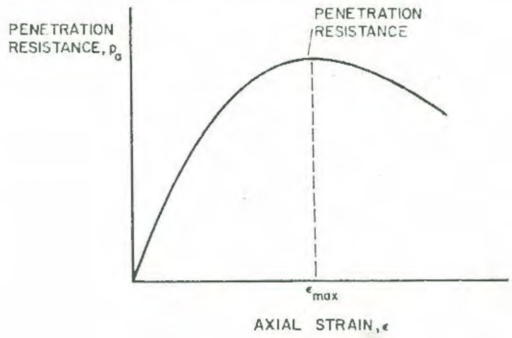

Figure 8 — Penetration resistance

Fig. 8. It can be seen that the penetration resistance increases with increasing axial deformation and reaches a peak value at an axial unit deformation equal to ε_{max}. This unit deformation will be larger than that corresponding to the peak point of the average stress-strain relationship as obtained from triaxial tests. The reason for this behavior is that the calculated penetration resistance is very sensitive to small variations of the friction angle ϕ_m.

Ackowledgement

The method described in this paper was developed in 1956 when the author was employed by Shell Development Company, Houston, Texas.

for a rough wedge which is pushed into a rock mass is shown in Fig. 7. As the wedge penetrates into the rock mass, the contact pressure p_c will increase as the deformation of the rock surrounding the wedge increases.

The contact pressure p_c can be expressed in terms of the mobilised cohesion c_m and the friction resistance ϕ_m if the deformations of the rock are known or assumed. These calculations become relatively simple if it is assumed that the deformations are uniformly distributed. For this particular case the penetration resistance can be calculated directly from Fig. 5 as a function of an equivalent axial strain. As the equivalent axial strain ε_a, the cohesion c_m and the friction angle ϕ_m are mobilised. With a knowledge of these two quantities, the penetration resistance can be calculated; the general relationship between penetration resistance and equivalent axial deformation is shown in

Figure 6—Penetration resistance

Fig. 6. It can be seen that the penetration resistance increases with increasing axial deformation and reaches a peak value at an axial deformation equal to ε_a. This axial deformation will be larger than that corresponding to the peak point of the average stress-strain relationship as obtained from triaxial tests. The reason for this behaviour is that the peak penetration resistance is very sensitive to small variations of the friction angle ϕ_m.

Acknowledgement

The work described in this paper was developed in ... and was financed by Shell Development Company, Houston, Texas.

Figure 5—Mobilisation of c_m and ϕ_m

shown in Fig. 5. It can be seen that the mobilised cohesion c_m increases very rapidly with increasing axial deformation and reaches a maximum value at a relatively small axial deformation. The friction resistance $\tan \phi_m$ increases relatively slowly with increasing axial deformation and reaches a maximum at a relatively large axial deformation.

The strain corresponding to the peak of a particular stress-strain curve will generally not coincide with either the strain at which the peak cohesion is mobilised or the strain at which the peak angle of internal friction is mobilised. The peak point of a particular stress-strain relationship will correspond to the strain at which the sum of the mobilised cohesion and the mobilised friction resistance reaches a maximum.

Penetration resistance of a wedge

The mobilised cohesion c_m and the mobilised friction resistance $\tan \phi_m$ can be used to predict the penetration resistance of a wedge. The idealised slip line pattern

Figure 7—[illegible]

Tensile strength of rock materials*

by BENGT B. BROMS

Director, Swedish Geotechnical Institute, Stockholm, Sweden

Tensile cracks are assumed to form in rock when the maximum tensile strength stress reaches the tensile strength as evaluated by the direct tension, the modulus of rupture or the Brazilian tests. However, several investigators have recognized that the tensile strength may be affected by a compression stress acting perpendicular to the direction of the maximum tensile stress. Some interaction relationship have been proposed. These interaction relationships are generally based on Griffith's or Mohr's theories of failure or on a stress invariant failure theory.

The different test methods and the differences in measured tensile strength are discussed herein.

A large number of different types of direct tension tests are used by different investigators. The test specimens have frequently been provided with enlarged ends to force failure to take place within the center section. The tensile strength of rock can also be estimated from modulus of rupture tests. These tests are in general carried out on prisms which are loaded at the third points. The tensile strength is usually calculated by assuming that the stresses at the failure section are distributed linearly over the cross-section.

The split cylinder or Brazilian test is used extensively to evaluate the tensile strength of rock. In this test cylinders are loaded along its diameter. The applied load is distributed over some width by inserting strips of wood, plywood, cork or fiberboard between the testing machine and the test specimens. The stress distribution at failure is generally evaluated by assuming that rock behaves as an ideal elastic material. The corresponding stress distribution in the axial and lateral directions along the vertical diameter is shown in Figs. 1 a and 1 b, respectively.

The axial compression stress (Fig. 1 a) reaches a maximum at two load points. It decreases rapidly with increasing distance from the load points and reaches a minimum at the center of the rock cylinder. The minimum compression stress is three times the constant lateral tensile stress, (Fig. 1 b). It should be noted that a concentrated lateral compression force is present at each load point. If the applied load is distributed over some width, the stress distribution will be modified at the load points. The stress change will however be small close to the center of the member.

Failure for the split cylinder test is indicated by the formation of a tensile crack close to the center of the test cylinders which spread towards the two load points. This behavior is in contradiction with that predicted by the Mohr's theory of failure or by a stress invariant failure theory.

The Mohr's stress circles describing the stress distribution for two elements located along the vertical diameter of a test specimen is shown in Fig. 2. The minimum principal stress (equal to the lateral maximum tensile stress) is the same for the two elements. The axial compression stress will however be smaller for element 1 than for element 2. Thus the stress circle for element 1 is located inside the stress circle corresponding to element 2. According to Mohr's theory of failure, the tensile cracks leading to failure should therefore initiate at the point which corresponds to the stress circle with the largest diameter. Thus, Mohr's failure theory predicts that failure should initiate at or close to the load points and should travel towards the center of the cylinder in contrast to available test data.

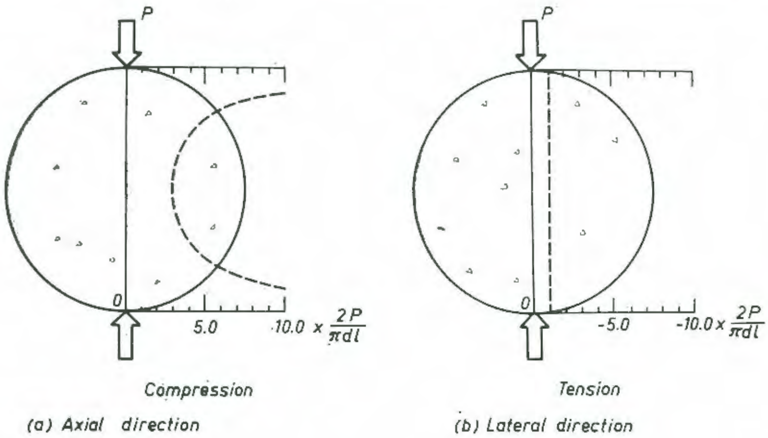

Fig. 1. Stress distribution in the Brazilian test

* Discussion on: Properties of Rocks and Rock Masses. Proc. Ist Congr. Int. Soc. Rock Mech., Lisbon 1966, Vol. 3.

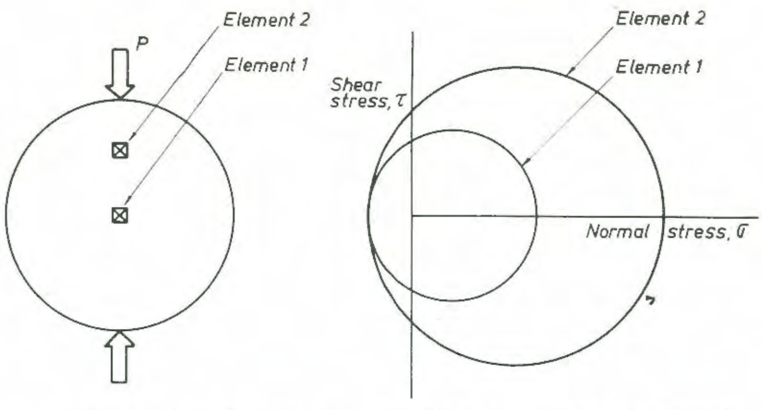

(a) Location of elements 1 and 2 (b) Stress distribution for elements 1 and 2

Fig. 2. Interpretation of the Brazilian test

The test results frequently indicate that the tensile strength evaluated from the Brazilian test or from modulus of rupture tests is higher than that determined from direct tension tests. The difference in tensile strength as measured by the modulus of rupture and the direct tension tests can at least partly be attributed to a non-linear, stress-strain relationship in tension. If, for example, this relationship is a parabola and the initial modulus of elasticity in tension is equal to that in compression, the actual maximum tensile stress will be only 72 percent of the elasticity calculated modulus of rupture.

The difference in tensile strength between the split cylinder and tbe direct tension test can be attributed partly to a difference in relative volume of rock subjected to the maximum tensile stress and partly to a difference in the stress conditions.

The lateral tensile stresses for the split cylinder test are the largest along the vertical diameter of the test member. At other sections located only a small horizontal distance away, the tension stresses are considerably smaller. At failure, the tensile cracks are forced to proceed along this vertical plane where the high tensile stresses are concentrated. A mineral particle located along this path will act as a local obstacle forcing and a propagating crack will either pass through the particle or to follow along its boundary. Both of these effects will cause an increase of the measured apparent tensile strength.

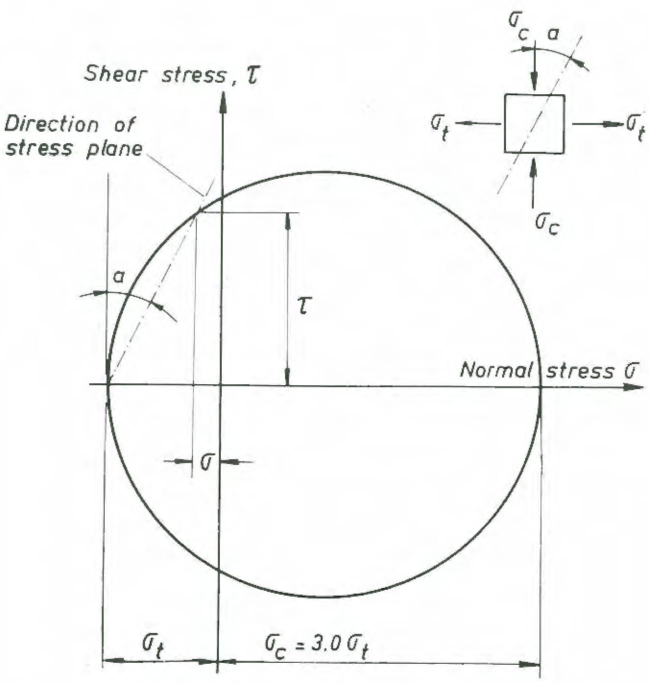

Fig. 3. Mohr's stress circle for the Brazilian test

The large vertical compressive stresses present at a Brazilian test probably also affect the tensile strength. At the center of the test cylinder, the vertical compressive stress is three times the horizontal tension stress. The resulting distribution of normal and shear stresses as determined from the Mohr's stress circle, is shown in Fig. 3. The maximum principal stress σ_c is the compression stress acting in the vertical direction. The minimum principal stress σ_t is the horizontal tension acting on the vertical diametrical plane. Normal and shear stresses equal to σ and τ respectively, will act on planes inclined at an angle ∞ from the vertical. It can be seen that the normal stress is highly sensitive to the inclination of the stress plane. When tbe inclination ∞ is equal to 30 degrees, the normal stress σ is equal to zero. When the inclination is larger than 30°, a compressive stress will act on the inclined plane. This compressive stress will prevent a crack from propagation along planes which are inclined at an angle larger than $\pm$ 30° from the vertical. Thus, the axial compression stress present in a split cylinder test forces the cracks to travel along the vertical diameter of the cylinder. Even slight meandering along weak paths is prevented by the stress field.

The tendency of forcing the tensile cracks to penetrate through rather than to pass around the individual aggregate particles will increase with increasing compressive stress. Thus, it is expected that for the split cylinder test, relatively few mineral particles will he fractured close to the center of the specimen where the compressive stress is low and that the number of fractured aggregate particles will increase with decreasing distance from the load points (as the compressive stress increases).

It is therefore expected that the tensile strength as measured by the split cylinder test will depend to a large extent on the tensile strength of the mineral particles (since the fracture surface will pass through a relatively large number of particles). Furthermore, it is expected that the tensile strength as measured by the modulus of rupture or direct tension tests will primarily he influenced by the bond strength of the mineral particles since the fracture surface will follow the surface of the individual mineral particles.

SÄRTRYCK OCH PRELIMINÄRA RAPPORTER

Reprints and preliminary reports

No.			Pris kr. (Sw. crs.)
1.	Views on the Stability of Clay Slopes. *J. Osterman*	1960	Out of print
2.	Aspects on Some Problems of Geotechnical Chemistry. *R. Söderblom*	1960	»
3.	Contributions to the Fifth International Conference on Soil Mechanics and Foundation Engineering, Paris 1961. Part I.	1961	»
	1. Research on the Texture of Granular Masses. *T. Kallstenius & W. Bergau*		
	2. Relationship between Apparent Angle of Friction — with Effective Stresses as Parameters — in Drained and in Consolidated-Undrained Triaxial Tests on Saturated Clay. Normally-Consolidated Clay. *S. Odenstad*		
	3. Development of two Modern Continuous Sounding Methods. *T. Kallstenius*		
	4. In Situ Determination of Horizontal Ground Movements. *T. Kallstenius & W. Bergau*		
4.	Contributions to the Fifth International Conference on Soil Mechanics and Foundation Engineering, Paris 1961. Part II.	1961	5:—
	Suggested Improvements in the Liquid Limit Test, with Reference to Flow Properties of Remoulded Clays. *R. Karlsson*		
5.	On Cohesive Soils and Their Flow Properties. *R. Karlsson*	1963	10:—
6.	Erosion Problems from Different Aspects.	1964	10:—
	1. Unorthodox Thoughts about Filter Criteria. *W. Kjellman*		
	2. Filters as Protection against Erosion. *P. A. Hedar*		
	3. Stability of Armour Layer of Uniform Stones in Running Water. *S. Andersson*		
	4. Some Laboratory Experiments on the Dispersion and Erosion of Clay Materials. *R. Söderblom*		
7.	Settlement Studies of Clay.	1964	10:—
	1. Influence of Lateral Movement in Clay Upon Settlements in Some Test Areas. *J. Osterman & G. Lindskog*		
	2. Consolidation Tests on Clay Subjected to Freezing and Thawing. *J. G. Stuart*		
8.	Studies on the Properties and Formation of Quick Clays. *J. Osterman*	1965	5:—
9.	Beräkning av pålar vid olika belastningsförhållanden. *B. Broms*	1965	30:—
	1. Beräkningsmetoder för sidobelastade pålar.		
	2. Brottlast för snett belastade pålar.		
	3. Beräkning av vertikala pålars bärförmåga.		
10.	Triaxial Tests on Thin-Walled Tubular Samples.	1965	5:—
	1. Effects of Rotation of the Principal Stress Axes and of the Intermediate Principal Stress on the Shear Strength. *B. Broms & A. O. Casbarian*		
	2. Analysis of the Triaxial Test-Cohesionless Soils. *B. Broms & A. K. Jamal*		
11.	Något om svensk geoteknisk forskning. *B. Broms*	1966	5:—
12.	Bärförmåga hos pålar slagna mot släntberg. *B. Broms*	1966	15:—
13.	Förankring av ledningar i jord. *B. Broms & O. Orrje*	1966	5:—
14.	Ultrasonic Dispersion of Clay Suspensions. *R. Pusch*	1966	5:—
15.	Investigation of Clay Microstructure by Using Ultra-Thin Sections. *R. Pusch*	1966	10:—
16.	Stability of Clay at Vertical Openings. *B. Broms & H. Bennermark*	1967	10:—

No.			Pris kr. (Sw. crs.)
17.	Om pålslagning och pålbärighet.	1967	5:—
	1. Dragsprickor i armerade betongpålar. *S. Sahlin*		
	2. Sprickbildning och utmattning vid slagning av armerade modellpålar av betong. *B-G. Hellers*		
	3. Bärighet hos släntberg vid statisk belastning av bergspets. Resultat av modellförsök. *S-E. Rehnman*		
	4. Negativ mantelfriktion. *B. H. Fellenius*		
	5. Grundläggning på korta pålar. Redogörelse för en försöksserie på NABO-pålar. *G. Fjelkner*		
	6. Krokiga pålars bärförmåga. *B. Broms*		
18.	Pålgruppers bärförmåga. *B. Broms*	1967	10:—
19.	Om stoppslagning av stödpålar. *L. Hellman*	1967	5:—
20.	Contribution to the First Congress of the International Society of Rock Mechanics, Lisbon 1966.	1967	5:—
	1. Anote on Strength Properties of Rock. *B. Broms*		
	2. Tensile Strength of Rock Materials. *B. Broms*		